High-order Accurate Solutions Using an Implicit Discontinuous Galerkin Method on Unstructured Meshes

Hee Dong LEE [1] and Oh Joon KWON[1]

1) *Department of Aerospace Engineering, KAIST, Daejeon 305-701, KOREA*

Corresponding Author: Oh Joon KWON, ojkwon@kaist.ac.kr

ABSTRACT

A high-order implicit discontinuous Galerkin flow solver for the two-dimensional Euler equations was developed on unstructured triangular meshes. Numerical tests for the supersonic vortex flow were conducted to estimate the convergence order of numerical solutions and to assess the effect of high-order representation of curved solid boundaries in discontinuous Galerkin methods. The flow around a 2-D circular cylinder was also numerically simulated for the demonstration of the efficiency of the high-order implicit discontinuous Galerkin method in obtaining steady state solutions. The numerical results showed that the implicit discontinuous Galerkin methods with a high-order representation of curved solid boundaries can be an efficient method to obtain very accurate numerical solutions on unstructured meshes.

INTRODUCTION

Recently, discontinuous Galerkin method(DGM) has experienced a resurgence of interest in various disciplines of numerical simulations on unstructured meshes[1]. DGM has advantageous features from both finite-element and finite-volume methods. In the case of DGM, high-order accuracy is achieved by increasing the degree of approximating polynomials without relying on extended stencils as in the classical finite-volume methods. Since the approximate solutions are represented by element-wise polynomials without inter-element continuity restriction, numerical flux schemes originally developed for finite-volume methods are used to determine unique flux values at elemental boundaries. Also, DGM maintains the compactness, regardless of the order of accuracy, because the required stencil is confined only to the neighbors of elemental boundaries. Owing to this favorable property, DGM is highly parallelizable and easily handles adaptive mesh strategies.

The DGM was originally considered by Reed and Hill[2] to solve a neutron transport problem and extended by Cockburn and Shu[3] for the nonlinear systems of hyperbolic conservation laws. They developed the Runge-Kutta discontinuous Galerkin method based on method of lines, in which the governing equations are first discretized for spatial variables by using DGM, then the semi-discrete ordinary differential equations are integrated in time with the aid of a TVD Runge-Kutta method. Even though the explicit Runge-Kutta Discontinuous Galerkin method has been widely used to obtain steady state solutions, the rate of convergence to steady solutions may become dramatically slow for large-scale simulations due to the fact that CFL stability condition is severely restricted as the degree of approximation polynomials increases and/or the mesh is refined. One way to overcome this difficulty is to use an implicit time integration method which has essentially no stability limitation.

In the present study, a high-order implicit discontinuous Galerkin flow solver for the two-dimensional Euler equations has been developed on unstructured meshes. The flow solver adopted a fully implicit method based on Euler backward differencing and linearization of the residuals to obtain steady solutions effectively. Two numerical tests are to be presented, which were selected to estimate the accuracy of numerical solutions and to assess the efficiency of the high-order implicit discontinuous Galerkin method in obtaining steady state solutions.

NUMERICAL METHODS

The governing equations in the present study are the two-dimensional Euler equations for compressible inviscid flows, which can be expressed in a conservative form as

$$\frac{\partial}{\partial t}\mathbf{U}(\mathbf{x},t)+\nabla\cdot\vec{\mathbf{F}}=0, \quad (\mathbf{x},t)\in\Omega\times(0,T) \tag{1}$$

where $\Omega\in R^2$ is an open domain with boundary $\partial\Omega\subset\bar{\Omega}$. Also, $\mathbf{U}$ and $\vec{\mathbf{F}}=\{\mathbf{F}_1,\mathbf{F}_2\}$ represent the vector of conservative flow variables and inviscid Euler fluxes, respectively.

To obtain a weak form of the governing equations, the conservation laws in Eq. (1) are multiplied by an arbitrary smooth function $\mathbf{W}$ and integrated by parts over the domain Ω:

$$\frac{\partial}{\partial t}\int_\Omega \mathbf{W}^T\mathbf{U}d\Omega+\int_{\partial\Omega}\mathbf{W}^T\left(\mathbf{n}^T\vec{\mathbf{F}}\right)dS-\int_\Omega\nabla\mathbf{W}^T\cdot\vec{\mathbf{F}}d\Omega=0 \quad \forall\mathbf{W} \tag{2}$$

where $\mathbf{n}$ denotes the outward unit normal vector to the boundary.

To discretize Eq. (2), both analytical solution $\mathbf{U}$ and arbitrary test function $\mathbf{W}$ are replaced by Galerkin finite-element approximation $\mathbf{U}_h$ and $\mathbf{W}_h$, respectively, which belong to the finite-element space V_h^p defined by

$$\begin{aligned} V_h^p &= \left\{\mathbf{v}\in\left[L_2(\Omega)\right]^4 : \mathbf{v}|_K\in(p_1,...,p_4)^T\right\} \\ p_i &\in P^p(K) \end{aligned} \tag{3}$$

where $P^p(K)$ is a discontinuous piecewise polynomial space of degree p defined on each element K. Then $\mathbf{U}_h$ and $\mathbf{W}_h$ can be expressed as

$$\mathbf{U}_h(\mathbf{x},t)=\sum_{l=1}^{N_{dof}}\hat{\mathbf{U}}_l(K,t)\phi_l(\mathbf{x}), \quad \mathbf{W}_h(\mathbf{x})=\sum_{l=1}^{N_{dof}}\hat{\mathbf{W}}_l(K)\phi_l(\mathbf{x}) \tag{4}$$

where N_{dof} is the number of degree of freedoms to represent the approximate solution in a form of truncated polynomial expansions and is given by $(k+1)(k+2)/2$ for two-dimensional elements. Since the approximate solution $\mathbf{U}_h$ is discontinuous across the element interfaces, the inviscid flux $\mathbf{n}^T\vec{\mathbf{F}}$ has to be replaced by a numerical flux $\mathbf{H}\left(\mathbf{U}_h^-,\mathbf{U}_h^+,\mathbf{n}\right)$, which depends on both inner and outer traces of $\mathbf{U}_h$ on ∂K and the unit outward normal vector $\mathbf{n}$ to the elemental boundary. In the present study, the numerical flux of Roe[4] originally developed for finite-volume methods was adopted. The discontinuous Galerkin formulation of the governing equations can be expressed for an arbitrary element K as follows:

$$\frac{\partial}{\partial t}\int_K\mathbf{W}_h^T\mathbf{U}_h d\Omega +\int_{\partial K}\mathbf{W}_h^T\mathbf{H}\left(\mathbf{U}_h^-,\mathbf{U}_h^+,\mathbf{n}\right)dS$$
$$-\int_K\nabla\mathbf{W}_h^T\cdot\vec{\mathbf{F}}d\Omega=0, \quad \forall\mathbf{W}_h\in V_h^p \tag{5}$$

By introducing the polynomial expansions for $\mathbf{U}_h$ and $\mathbf{W}_h$ as in Eq. (4) into Eq. (5), a set of equations for the coefficients $\hat{U}_{jl}$ is obtained:

$$\int_K \phi_l \phi_m d\Omega \, \delta_{ij} \frac{d}{dt} \hat{U}_{jm} = -\int_{\partial K} \phi_l H_i \left(\mathbf{U}_h^-, \mathbf{U}_h^+, \mathbf{n} \right) dS + \int_K \nabla \phi_l \cdot \vec{F}_i d\Omega \tag{6}$$

where $i, j = \{1, ..., 4\}$ represent indices of the four Euler equations in two dimensions, and $l, m = \{1, ..., N_{dof}\}$ denote indices of the basis functions and the coefficients of the truncated polynomial expansions. Eq. (6) can be rewritten as follows:

$$m_{lm} \delta_{ij} \frac{d\hat{U}_{jm}^-}{dt} = R_{il} \left(\mathbf{U}_h^-, \mathbf{U}_h^+ \right) \tag{7}$$

where

$$\begin{aligned} m_{lm} &= \int_K \phi_l^- \phi_m^- d\Omega \\ R_{il} &= -\int_{\partial K} \phi_l H_i \left(\mathbf{U}_h^-, \mathbf{U}_h^+, \mathbf{n} \right) dS + \int_K \nabla \phi_l \cdot \vec{F}_i d\Omega \end{aligned} \tag{8}$$

Here, $-$ and $+$ denote the quantities inside and outside of K. This scheme is called as a discontinuous Galerkin method of degree p, or 'DG(p) method', which has an order of accuracy of $p+1$ [5].

Once spatial discretization is completed, a set of ordinary differential equations is obtained as in Eq. (7). These ordinary differential equations can be integrated in time by using either explicit or implicit methods. In the present study, a fully implicit method based on the backward Euler time integration was applied to Eq. (7) as

$$m_{lm} \delta_{ij} \frac{\hat{U}_{jm}^- \big|^{n+1} - \hat{U}_{jm}^- \big|^n}{\Delta t} = R_{il}^{n+1} \left(\mathbf{U}_h^-, \mathbf{U}_h^+ \right) \tag{9}$$

The right-hand side is now linearized by using the Taylor expansion as

$$R_{il}^{n+1} \left(\mathbf{U}_h^-, \mathbf{U}_h^+ \right) \approx R_{il}^n + \frac{\partial R_{il}}{\partial \hat{U}_{jm}^-} \bigg|^n \Delta \hat{U}_{jm}^- + \frac{\partial R_{il}}{\partial \hat{U}_{jm}^+} \bigg|^n \Delta \hat{U}_{jm}^+ \tag{10}$$

where $\Delta \hat{U}$ indicates $\hat{U}^{n+1} - \hat{U}^n$. The Jacobians of R_{il} to $\hat{U}_{jm}$ can be derived from Eq. (8) as

$$\begin{aligned} \frac{\partial R_{il}}{\partial \hat{U}_{jm}^-} &= -\int_{\partial K} \phi_l^- \phi_m^- \frac{\partial H_i}{\partial U_j^-} dS + \int_K \phi_m^- \left(\frac{\partial \phi_l^-}{\partial x_1} \frac{\partial F_{1i}}{\partial U_j^-} + \frac{\partial \phi_l^-}{\partial x_2} \frac{\partial F_{2i}}{\partial U_j^-} \right) d\Omega \\ \frac{\partial R_{il}}{\partial \hat{U}_{jm}^+} &= -\int_{\partial K} \phi_l^- \phi_m^+ \frac{\partial H_i}{\partial U_j^+} dS \end{aligned} \tag{11}$$

Then, Eq. (7) becomes

$$\left(m_{lm} \frac{\delta_{ij}}{\Delta t} - \frac{\partial R_{il}}{\partial \hat{U}_{jm}^-} \bigg|^n \right) \Delta \hat{U}_{jm}^- - \frac{\partial R_{il}}{\partial \hat{U}_{jm}^+} \bigg|^n \Delta \hat{U}_{jm}^+ = R_{il}^n \tag{12}$$

which can be rewritten in a matrix form for all elements in the mesh:

$$\mathbf{A} \Delta \mathbf{U} = \mathbf{R} \tag{13}$$

where the coefficient matrix $\mathbf{A}$ is a very sparse block matrix which is consisted of one diagonal block and three off-diagonal blocks for a triangular element. Each block is a square matrix having $4N_{dof} \times 4N_{dof}$ entities. The linear system of equations is solved at each time step by using a point Gauss-Seidel method.

NUMERICAL RESULTS

Numerical tests for two smooth flows were conducted to estimate the convergence order of numerical solutions and to assess the efficiency of the present high-order implicit discontinuous Galerkin method in obtaining steady solution. The first test was made for an inviscid, isentropic, supersonic flow in a quarter-circular annulus[6], where analytic solutions are available. The inner and outer radii were taken to be 2 and 3, respectively, and the Mach number at the inner radius was set to 2.0. The radial velocity of the flow is inversely proportional to radius and the density is given by

$$\rho = \rho_i \left[1 + \frac{\gamma - 1}{2} M_i^2 \left(1 - \frac{r_i^2}{r^2} \right) \right]^{\frac{1}{\gamma - 1}} \tag{14}$$

where, M_i and r_i denote Mach number and radius at the inner boundary.

Four unstructured meshes containing 230, 908, 3628, 14513 triangular elements were used for the computations. Figure 1 shows L2 norm of numerical errors in density with respect to
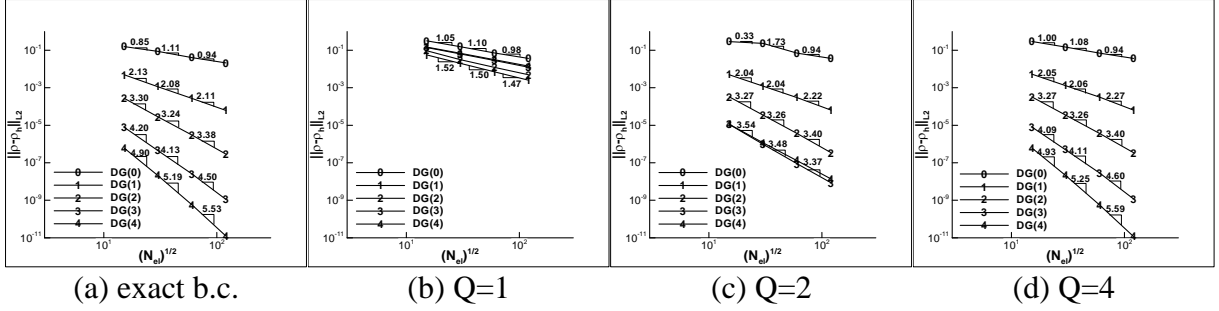

(a) exact b.c. (b) Q=1 (c) Q=2 (d) Q=4

Figure 1. Convergence of errors in density for the supersonic vortex flow
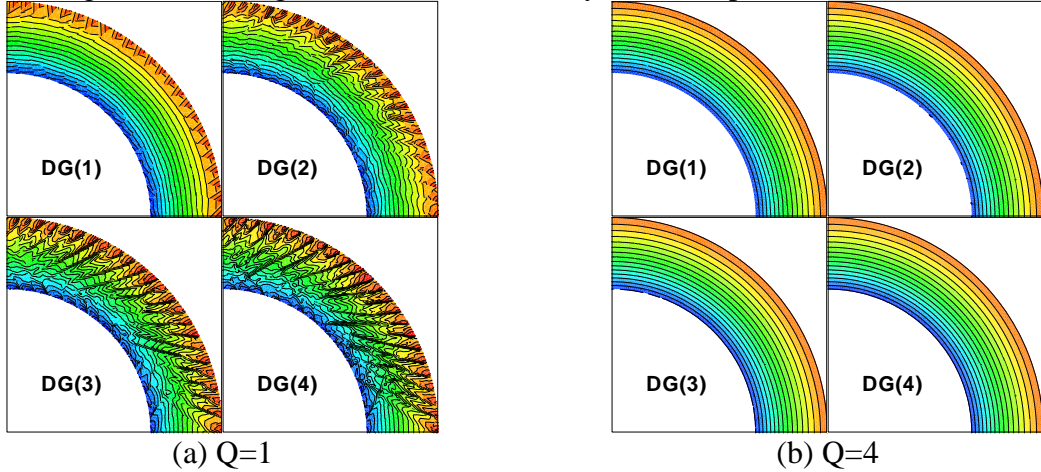

(a) Q=1 (b) Q=4

Figure 2. Density contours for the supersonic vortex flow($N_{el} = 230$)
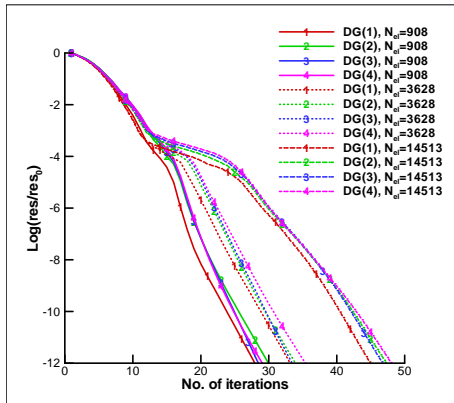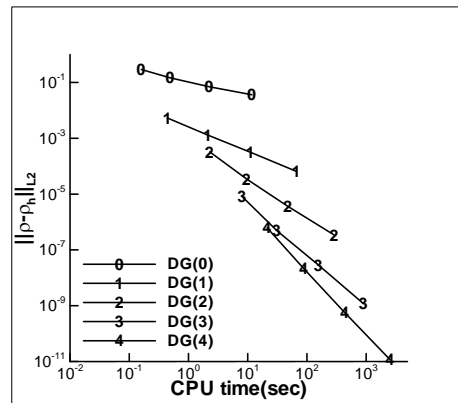

Figure 3. Residual convergence

Figure 4. Elapsed CPU time vs. errors

28

the grid size depending on the types of boundary approximation. The grid size is represented by using the square root of number of elements. First, calculations with exact boundary conditions were made to remove the effect of boundary conditions and the estimated order of accuracy is shown in Figure 1(a). It can be observed that the optimal order of error convergence, $p+1$ for DG(p) method, was achieved by using the present implicit discontinuous Galerkin solver. Next, numerical tests with imposing the slip boundary condition to the curved solid walls at the inner and outer radii were conducted. The order of accuracy was measured for the approximation of the curved boundaries by employing piecewise linear through quartic polynomials. The estimated orders of accuracy are shown in Figure 1 (b) to (d). For DG(0) method, the optimal order of accuracy was obtained regardless of the degree of polynomials, Q, for the curved boundary approximation. As indicated by Bassi and Rebay[7], however, it was observed that the linear approximation of the curved boundaries(Q=1) leads to dramatic loss of accuracy and even to unphysical solutions for high-order DG methods as shown in Figure 2. When the quadratic boundary approximation was used for the curved boundaries(Q=2), the optimum order of accuracy was achieved up to the DG(2) method. For the case of cubic polynomial approximation(Q=3), the estimated order of accuracy was similar to the case of quadratic approximation. To obtain optimum accuracy up to the DG(4) method, it was necessary that a quartic polynomial approximation be used in the present study.

Residual convergence histories from initial conditions to the steady state solutions are shown in Figure 3. For a given mesh, the rates of residual convergence are similar regardless of accuracy due to the fact that the Jacobians for the implicit time integration were determined with the same accuracy as residuals. Figure 4 shows elapsed computational time and density errors of the steady solutions which were obtained by converging the residuals to machine zero. It is clearly indicated that higher-order implicit DG methods are more efficient to achieve a given level of errors for the steady flow computations.

The second test case was a subsonic flow around a circular cylinder at a Mach number of 0.3. Steady computations were made on two unstructured meshes containing 352 and 1272 triangular elements. On the two meshes, the circular cylinder was enclosed with 12 and 24
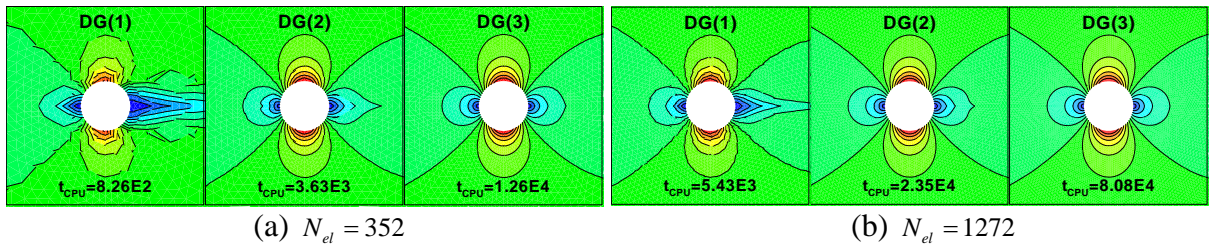

(a) $N_{el} = 352$ (b) $N_{el} = 1272$

Figure 5. Mach contours and elapsed CPU time for the calculations on two unstructured meshes.

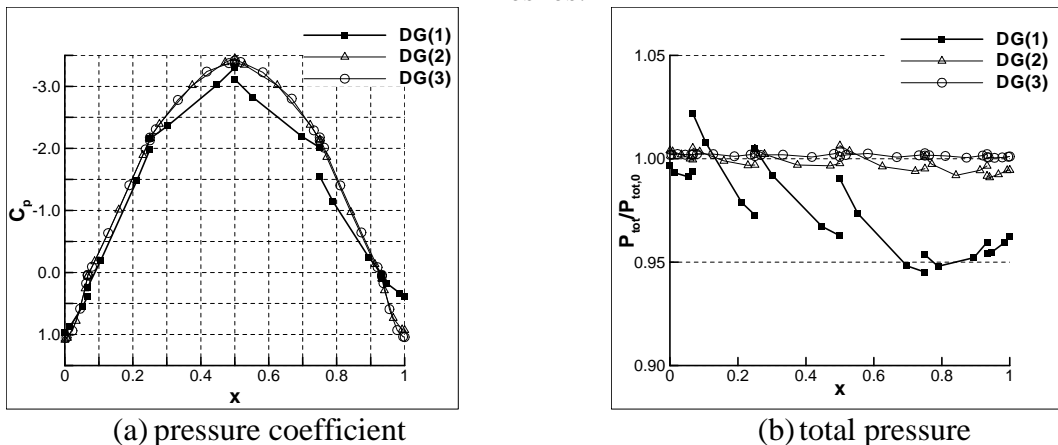(a) pressure coefficient   (b) total pressure

Figure 6. Pressure coefficient and total pressure distributions around a circular cylinder

curved triangular elements approximated by piecewise quadratic polynomials. Figure 5 represents Mach contours and elapsed CPU time for DG(1) through DG(3) calculations on two unstructured meshes. For the lower-order calculations on the coarser mesh, unphysical wakes were produced due to the inherent dissipation of the numerical methods. This wakes were reduced as the order of accuracy increased and the mesh was refined. And it was also found that higher-order DG methods are more efficient in terms of computational time needed for achieving the same level of accuracy in numerical solutions. The accuracy of the present method could also be verified by comparing the distributions of pressure coefficient and total pressure obtained on the coarse mesh for DG(1) through DG(3) computations as shown in Figure 6. It shows that the pressure at the rear of the cylinder is recovered and the loss of total pressure decreases drastically as the order of accuracy increases.

CONCLUSIONS

A high-order implicit discontinuous Galerkin flow solver for the two-dimensional Euler equations has been developed on unstructured triangular meshes. The flow solver adopted a fully implicit method based on Euler backward differencing and linearization of the residuals to obtain steady solutions effectively. Numerical tests for the supersonic vortex flow were conducted to estimate the accuracy of numerical solutions and to assess the effect of high-order representation of curved solid boundaries in discontinuous Galerkin methods. The flow around a 2-D circular cylinder was also numerically simulated for the demonstration of the efficiency of the high-order implicit discontinuous Galerkin method in obtaining steady state solutions. The numerical results showed that the implicit discontinuous Galerkin methods with a high-order representation of curved solid boundaries can be an effective method to obtain very accurate numerical solutions on unstructured meshes.

REFERENCES

1. Cockburn, B., Karniadakis, G., and Shu, C.W.(eds.) *Discontinuous Galerkin Methods: Theory, Computation, and Applications*, Lecture Notes in Computational Science and Engineering, Springer, NY, 1999.
2. Reed, W. H. and Hill, T. R., "Triangular Mesh Methods for the Neutron Transport Equation," *Los Alamos Scientific Laboratory Report LA-UR-73-479*, 1973.
3. Cockburn, B. and Shu, C. W., "The Runge-Kutta Discontinuous Galerkin Finite Element Method for Conservation Laws Ⅴ: Multidimensional Systems," *Journal of Computational Physics*, Vol. 141, 1998, pp. 199-224.
4. Roe, P. L., "Approximate Riemann Solvers, Parametric Vectors, and Difference Scheme," *Journal of Computational Physics*, Vol. 43, 1981, pp. 357-372.
5. Hartmann, R. "Discontinuous Galerkin methods for compressible flows: higher order accuracy, error estimation and adaptivity," *VKI LS 2006-01: CFD - Higher Order Discretization Methods*, Belgium. 2005.
6. Ollivier-Gooch, C. F., "High-Order ENO Schemes for Unstructured Meshes Based on Least-Squares Reconstruction," *AIAA* Paper 97-0540, 1997.
7. Bassi, F. and Rebay, S., "High-order accurate discontinuous finite element solution of the 2D Euler equations," *Journal of Computational Physics*, Vol. 138, 1997, pp 251-285.